

## PAPER

[View Article Online](#)  
[View Journal](#) | [View Issue](#)Cite this: *Mater. Adv.*, 2023,  
4, 4226A database to select affordable MOFs for  
volumetric hydrogen cryoadsorption considering  
the cost of their linkers†‡Jose A. Villajos,<sup>a</sup> Martin Bienert,<sup>b</sup> Nikita Gugin,<sup>c</sup> Franziska Emmerling<sup>d</sup>  
and Michael Maiwald<sup>e</sup>

Physical adsorption at cryogenic temperature (cryoadsorption) is a reversible mechanism that can reduce the pressure of conventional compressed gas storage systems. Metal–organic framework (MOF) materials are remarkable candidates due to the combination of high specific surface area and density which, in some cases, provide a high volumetric storage capacity. However, such extensive use of MOFs for this application requires the selection of affordable structures, easy to produce and made from feasible metallic and organic components. Herein, we introduce a MOF database detailing the crystallographic and porous properties of 3600 existing MOFs made from industrially relevant metals and their organic composition. The comparison of the available minimum costs of linkers allowed the creation of a database to select affordable structures with high potential for volumetric hydrogen storage by cryoadsorption, considering their composition based on individual or mixed building blocks. A user interface, available online, facilitates the selection of MOFs based on the properties or names of structures and linkers.

Received 20th June 2023,  
Accepted 16th August 2023

DOI: 10.1039/d3ma00315a

[rsc.li/materials-advances](https://rsc.li/materials-advances)

## Introduction

Generating green hydrogen as an energy carrier is a versatile solution to store electricity derived from unsteady renewable sources, contributing to decarbonising activity in sectors like industry and transport.<sup>1</sup> However, despite the advantages of hydrogen as an energy carrier, its deployment has limitations,

such as the low energy storage density, which requires compressing the gas up to 1000 bar or cooling it down for its liquefaction at  $-253\text{ }^{\circ}\text{C}$ .<sup>2,3</sup>

Physical adsorption (physisorption) is an alternative storage mechanism in which hydrogen molecules cover solid surfaces due to van der Waals, electrostatic, or orbital interactions without forming new chemical bonds.<sup>4</sup> Physisorption allows fast and reversible gas loading compared to chemical storage methods like using metal hydrides or liquid carriers since the interaction energies between the hydrogen molecules and the adsorbents are comparably low.<sup>5</sup> For this reason, this mechanism requires cryogenic temperatures of *ca.*  $-196\text{ }^{\circ}\text{C}$  to increase the volumetric density of the compressed gas at the same pressure and temperature.<sup>6</sup> However, the necessary liquid nitrogen is also used during the hydrogen liquefaction process, which is considered a viable option for large-scale storage or transportation.<sup>3</sup>

Porous materials such as zeolites and carbons have been intensively investigated for the cryoadsorption of hydrogen as a storage solution.<sup>7</sup> Ultraporous materials like COFs (covalent organic frameworks) and MOFs (metal–organic frameworks) provide a higher storage uptake because of their large surface area, high void fraction, and comparably lower density. MOFs used for hydrogen adsorption are crystalline coordination polymers with three-dimensional porosity where organic molecules link metal atoms or clusters by electron–donor groups.<sup>8</sup>

<sup>a</sup> Hydrogen and Power-to-x, Iberian Energy Storage Research Centre (CIIAE), Polígono 13, Parcela 31, “El Cuartillo”, Cáceres, Spain.

E-mail: jose.villajos@ciiae.org

<sup>b</sup> Materials Chemistry, Bundesanstalt für Materialforschung und -prüfung (BAM), Richard-Willstätter Str. 11, Berlin, Germany. E-mail: Martin.bienert@bam.de

<sup>c</sup> Analytical Chemistry, Reference Materials, Bundesanstalt für Materialforschung und -prüfung (BAM), Richard-Willstätter Str. 11, Berlin, Germany.

E-mail: Nikita.gugin@bam.de

<sup>d</sup> Materials Chemistry, Bundesanstalt für Materialforschung und -prüfung (BAM), Richard-Willstätter Str. 11, Berlin, Germany.

E-mail: Franziska.emmerling@bam.de

<sup>e</sup> Analytical Chemistry, Reference Materials, Bundesanstalt für Materialforschung und -prüfung (BAM), Richard-Willstätter Str. 11, Berlin, Germany.

E-mail: Michael.maiwald@bam.de

† It is with great sorrow that we dedicate this manuscript to the memory of Dr. Michael Maiwald. As a highly regarded physical chemist, he led the Division of Process Analytics at the Federal Institute for Materials Research and Testing (BAM). His kind-heartedness, integrity, and exceptional leadership have made a lasting and positive impact on us all.

‡ Electronic supplementary information (ESI) available. See DOI: <https://doi.org/10.1039/d3ma00315a>

The great variability of metals and organic linkers and their possible geometries and topologies resulted in more than 70 000 MOF structures that have been experimentally synthesised.<sup>9</sup>

The initially promising hydrogen uptake of the crystalline Zn-terephthalate MOF-5 of up to 7.1 wt% at  $-196\text{ }^{\circ}\text{C}$  and 40 bar<sup>10</sup> has been surpassed by materials such as NU-100 and MOF-210, reaching nearly 15 wt% at  $-196\text{ }^{\circ}\text{C}$  and 80 bar.<sup>11</sup> However, a high gravimetric hydrogen uptake in ultra-porous materials is not necessarily related to a high volumetric uptake due to their extremely low density. These two properties (specific surface area and density) must be balanced to show both high gravimetric and volumetric storage densities.<sup>12,13</sup> According to experimental measurements, some MOF structures like MOF-5, MOF-177, MOF-205, MOF-210, IRMOF-20, Mn-BTT, SNU-5, UCMCM-150, some NOTT-X materials (X: 101–103 and 110–115), PCN-11, PCN-46, PCN-51, and JUC-62 could simultaneously fulfil the gravimetric and volumetric DOE goals for 2025 of 5.5 wt% and  $40\text{ g L}^{-1}$  operating at  $-196\text{ }^{\circ}\text{C}$ .<sup>14–16</sup> In addition, hypothetical MOF structures also show potential to overcome the storage capacity goals as storage and usable gravimetric and volumetric capacities and indicate the direction to follow concerning composition and structure for the synthesis of new materials.<sup>17</sup>

MOFs have theoretically and experimentally outperformed some state-of-the-art materials for many applications. However,

they are currently expensive to produce, limiting their large-scale use.<sup>18</sup> Besides solvents, catalysts, structuring agents, obtention pathways, and the reaction yield to the final product, the organic and metallic compositions of MOFs influence their final cost and industrial feasibility, especially for bulky applications like hydrogen storage.<sup>19,20</sup> Reagents' availability, cost, ease of procurement, handling and even strategic or environmental constraints vary amongst metallic and organic starting materials. Moreover, some organic linkers are not commercially available and require specific multi-step chemical synthesis pathways.

Since the cost of the MOFs needs to be calculated specifically for each case, by evaluating the specific synthesis conditions, the use of solvents, or the price of the specific metal source, the organic and metallic composition could be used to compare the feasibility of structures fulfilling an operation requirement like, for example, hydrogen uptake, considering this selection as a general guide. The actual chemical composition of experimentally synthesised MOF materials is available in the Cambridge structural database (CSD) and can be extracted using provided algorithms.<sup>21</sup>

In this work, we collect the chemical composition of *ca.* 3500 MOF structures from the 2019 CoRE MOF database<sup>22,23</sup> with higher volumetric hydrogen storage capacity than  $40\text{ g L}^{-1}$  at  $-196\text{ }^{\circ}\text{C}$  and 100 bar, made from abundant and industrially relevant metals (see Fig. 1). The cost of the metallic precursors

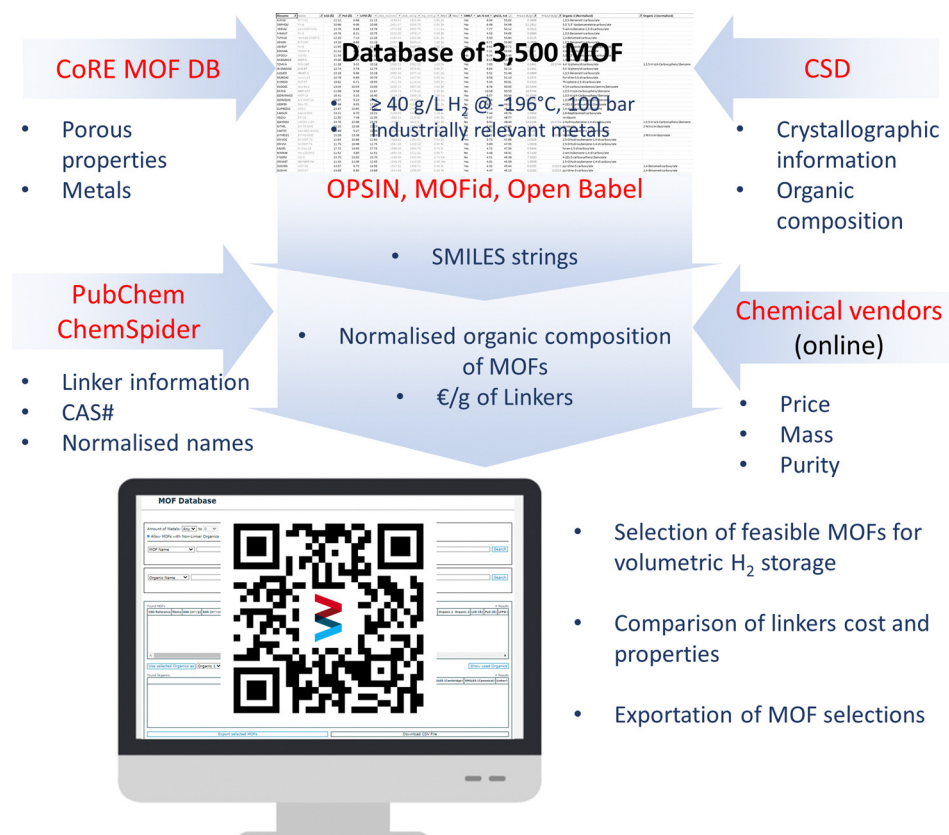


Fig. 1 Development of the database of feasible MOFs.



was not compared, since they are specific for each material and, in some cases, for the used synthetic conditions. The organic composition was collected and normalised by combining the reported procedures and an own algorithm, generating a list of potentially feasible linkers to produce MOFs on a large scale. Finally, we selected potential MOF structures for hydrogen storage by cryoadsorption involving up to two metals and two linkers. In addition, we made available a user interface that allows for creating customised selections of MOFs, having the properties of structures or linkers. Although this database was developed with hydrogen adsorption properties in mind, it could also be applied for selecting materials potentially useful for other applications where a combination of porosity, crystalline properties, and chemical composition is targeted, bearing in mind the nature of used metals and cost of the organic linkers.

## Methods and calculations

To elaborate this database, 3786 MOF structures with the potential to store a total volumetric uptake of at least  $40 \text{ g L}^{-1}$  from the CoRE MOF ASR 2019 (computational-ready experimental MOFs, all solvents removed) were selected. The calculated values of gravimetric and volumetric accessible areas, pore volume, void fraction, and density are collected in this database, along with the metallic composition and the potential presence of open metallic sites (OMS).<sup>23</sup> For this selection, only affordable and abundant metals in the Earth's crust were considered, like Al, Ca, Cd, Cr, Cu, Fe, Li, Mg, Mn, Mo, Na, Ni, Si, Sn, Sr, Ti, V, Zn, and Zr. The estimation of the storage capacity of each material is described in Section S1.2 of the ESI† and is based on a previously reported procedure not involving simulation.<sup>24</sup>

The organic composition of MOFs is neither defined in the CoRE MOF database<sup>23</sup> nor in the CSD MOF subset.<sup>9</sup> The chemical composition of the MOF structures in this database was directly obtained from the Cambridge Structure Database (CSD)<sup>9</sup> by using the software ConQuest (under the license of CCDC) (see details in Section S1.1 of the ESI†). Finally, the names of the identified organic compounds were normalised, and unique names and CAS numbers were assigned.

In order to find the price of the organic linkers and secure that the price applies to the same substance even appearing with different names (e.g., terephthalic or 1,4-benzenedicarboxylic acid), the organic components were identified using SMILES strings, CAS numbers, and using a normalised name (see details in Section S1.3 of the ESI†). In total, 1868 of the chemicals' names were converted into their corresponding SMILES strings. From this, 747 compounds were identified with their CAS numbers and finally classified as linkers or non-linkers. 598 substances were defined as linkers, and the prices of 510 substances were found online, finally selecting the minimum available price-per-gram for comparison.

A Python-based user interface was created to select MOF structures according to their crystalline or porous properties, hydrogen uptake, metallic and organic composition, number of

components, or specific chemical groups in their linkers (see Section S2 of the ESI† for more details). A version of this tool is available free of cost at <https://mofdb-bam.de>.

## Results and discussion

The selection of the materials focused on the volumetric hydrogen uptake of the MOF structures at  $-196^\circ\text{C}$  and 100 bar, which was estimated by our previously reported straightforward tool predicting the hydrogen uptake with 8% of average relative standard deviation with respect to calculated values by molecular simulation.<sup>24</sup> This tool is only valid for estimations at  $-196^\circ\text{C}$  and higher pressure values than that required for the saturation of the materials' surface with adsorbate molecules. The usable uptake, which consists of the difference between the stored amount at high pressure and the remaining adsorbed gas at low pressure (typically 5 bar), is more relevant for operation than the uptake itself of the adsorption system. However, calculating the remaining amount of gas at such a low-pressure value needs molecular simulation of the hydrogen uptake. This is out of the possibilities of the estimation procedure and the scope of this work. Therefore, we assumed a temperature-pressure swing operation, e.g., from  $-196^\circ\text{C}$  and 100 bar to  $-113^\circ\text{C}$  and 5 bar, for which 95–99% of the stored amount is reversibly recovered.<sup>25</sup> Besides, the calculation of the hydrogen uptake is based on a specific estimation of the porous properties, as well as density values considering the complete removal of extra-framework molecules as well as coordinated non-linker species for the creation of open metallic sites, both performed during the creation of the CoRE MOF database. However, a different degree of removal of these molecules may vary the porous properties of MOFs since it affects the free volume within the material. Besides, removing these species could vary their structures by inducing phase transformations that modify the porous properties and hence hydrogen uptakes. For these reasons, and similar to the calculations using any computational estimation, e.g., machine-learning, or molecular simulation, the predicted values herein must be experimentally validated.

The information in the database compared the composition of the selected MOFs and identified the most common building blocks. Zn is the most frequently used metal in these 3536 MOFs, with 1195 derived deposited MOF structures (see the ESI† for details about the selection procedure). 744 of these structures potentially exhibit open metallic sites (OMS), preferential adsorption sites for gases like hydrogen.<sup>26,27</sup> The second most-used metal is Cu with 940 structures. This noble metal is included in the database due to its industrial importance. From this selection, 845 materials show potential OMS. MOFs made from toxic metals like Be or Hg are not considered, except the 453 MOFs from Cd, a toxic metal cheaper than Cu. Cd can be obtained from Ni-MH batteries wastewater and solar cells recycling, so these MOFs could potentially help to reuse this metal's waste. Other attractive options are Fe, a cheap metal that can be reused from recycling scraps, and Mg, Mn,



Cr, and Zr. This last metal (Zr) is present in some materials with the highest structural stability among MOFs, like UIO-66.<sup>28</sup>

The costs of *ca.* 500 identified linkers in this database were found on the websites of the chemical suppliers. Among the different available prices for each substance from the different suppliers, we selected the lowest price-per-gram for this comparison, usually reached by the largest packed amount. The cost of the identified linkers varies in a  $10^7$  order of magnitude, from 0.01 € g<sup>-1</sup> for fumaric acid (H<sub>2</sub>FA), which can be purchased on a kg-scale, to 162 540 € g<sup>-1</sup> for 2-pyridin-4-yl-1*H*-imidazole-4,5-dicarboxylic acid, only available for shipping on a mg-scale. Examples of cheap linkers for the current production of commercially available MOFs are 1,4-benzenedicarboxylic acid (H<sub>2</sub>BDC) in MOF-5, 2-aminobenzene-1,4-dicarboxylic acid (H<sub>2</sub>NBDC) in MIL-53, 1,3,5-benzenetricarboxylic acid (H<sub>3</sub>BTC) in HKUST-1, H<sub>2</sub>FA in Al-fumarate, and 2-methylimidazole (HMeIm) in ZIF-8. More expensive substances like 1,3,5-tris(4-carboxyphenyl)benzene (H<sub>3</sub>BTB) and 3,3',5,5'-azobenzene-tetracarboxylic acid (H<sub>4</sub>AzBTC) can be found in commercially available materials MOF-177 and PCN-250(Fe), respectively.

Fig. 2 compares the corresponding minimum hydrogen storage density for MOFs made from these linkers, considering structures with only one linker and one metal without non-linker organic molecules (*e.g.*, ammonium derivatives, monocarboxylic acids like benzoic acid, naphthalene, phenol...) that can act as SDAs, template molecules, charge-compensating ions, or capping agents. This comparison shows that higher minimum volumetric storage density values are generally reached in MOFs constructed from more expensive linkers. In general, cheap linkers are more frequently used in synthesising MOFs, often resulting in materials with lower surface area, finally reducing the average storage uptake as shown in Fig. 2. On the other hand, more expensive linkers are often used to synthesise targeted MOFs with enlarged surfaces by following

the principles of reticular chemistry.<sup>29</sup> However, the volumetric area of MOFs, which is related to volumetric hydrogen uptake,<sup>13</sup> depends on the specific combination of surface area and density of materials. Therefore, it is possible to achieve a high volumetric storage density in materials with relatively low surface area and high density by using the cheapest linkers. In our selections, we assumed the upper limit for linkers' cost by referencing the most expensive substance used in commercially available MOFs, the linker H<sub>4</sub>AzBTC. However, further optimisation of the linkers' syntheses is necessary for their industrial production. For instance, linkers cheaper than 10 \$ kg<sup>-1</sup> are necessary to limit the MOF cost below 70 \$ kg<sup>-1</sup> for methane storage.<sup>19</sup>

Fig. 3 shows a comparison of the hydrogen uptake calculated for the MOFs built from individual linkers cheaper than 10 € g<sup>-1</sup>, considering MOFs identified with a common name (different to the CSD reference). The majority of these have proven their permanent porosity. The highest uptake using the cheapest linker is the material MIL-88A, or Fe-FA, for which higher volumetric uptake was calculated compared to its isostructural material MIL-88B (Fe-BDC) due to the smaller pore size and higher density.<sup>30</sup> Lower predicted uptake with a similar cost of the linker was calculated for material CAU-10 or Al-IA, an ultramicroporous material from trivalent Al and isophthalic acid with high stability and permanent porosity. However, the measured hydrogen uptake was lower for this material, considering the actual density of the powders.<sup>31</sup> The material CPM-201 or Mg-BDC shows permanent porosity and could store up to 53 g L<sup>-1</sup> of hydrogen after the removal of the dimethylacetamide molecules coordinated to Mg atoms in the cluster.<sup>32</sup> In the same cost-range, the materials MOF-5 and MIL-88B are found, whose permanent porosity has also been corroborated. With a higher linker cost, material polyMOP-NH<sub>2</sub> or Cu<sub>7</sub>-NIA<sub>6</sub> is a metal-organic polyhedral which could store 54 g L<sup>-1</sup>, showing OMS on their paddle-wheel metallic clusters. Materials JUC-133 (Cd<sub>5</sub>-BTC<sub>4</sub>) and FJI-3 (Zn<sub>5</sub>-BTC<sub>3</sub>) store comparable amounts of hydrogen but are made from comparably more expensive linkers.

There are several additional structures in the database for which only the CSD reference code is available, with potential hydrogen uptake higher than 40 g L<sup>-1</sup>. Fig. S3 in the ESI† shows the hydrogen uptake of the deposited MOFs from individual linkers cheaper than H<sub>4</sub>AzBTC, the most expensive linker used among commercially available MOFs. The material Cd<sub>2</sub>-BTC (CSD code QISNIR) shows the highest volumetric uptake among the selection with 65.1 g L<sup>-1</sup>. In the dimeric metallic cluster of this compound, three of the eight coordination positions of each octahedron are occupied by dimethylacetamide molecules, which are completely removed to calculate the porous properties of the structure. However, this removal could indeed drive a crystal-phase transition, potentially resulting in the collapse of its pore structure.<sup>33</sup> Therefore, the actual hydrogen uptake of this MOF may be completely different.

Tables from S2 to S15 in the ESI† display the porous properties, composition and hydrogen uptake of MOFs constructed from one linker and a hydrogen uptake higher than 40 g L<sup>-1</sup>.

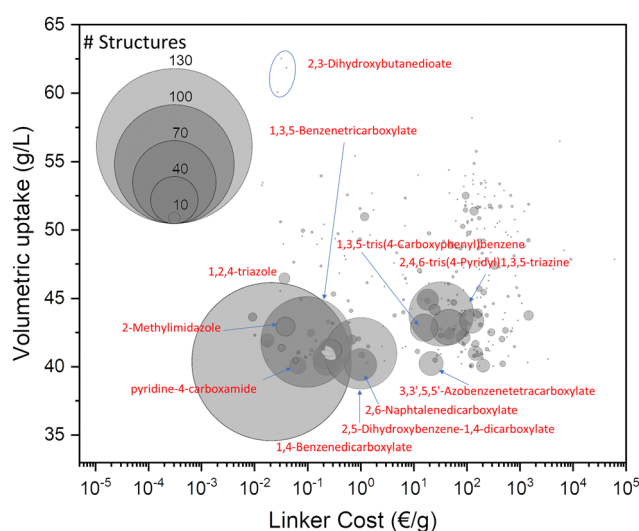


Fig. 2 Minimum H<sub>2</sub> storage density at -196 °C and 100 bar achieved for 1210 MOFs as a function of the cost of their linkers. The circles' centres correspond to the minimum H<sub>2</sub> uptake and diameter to the deposited number of structures.





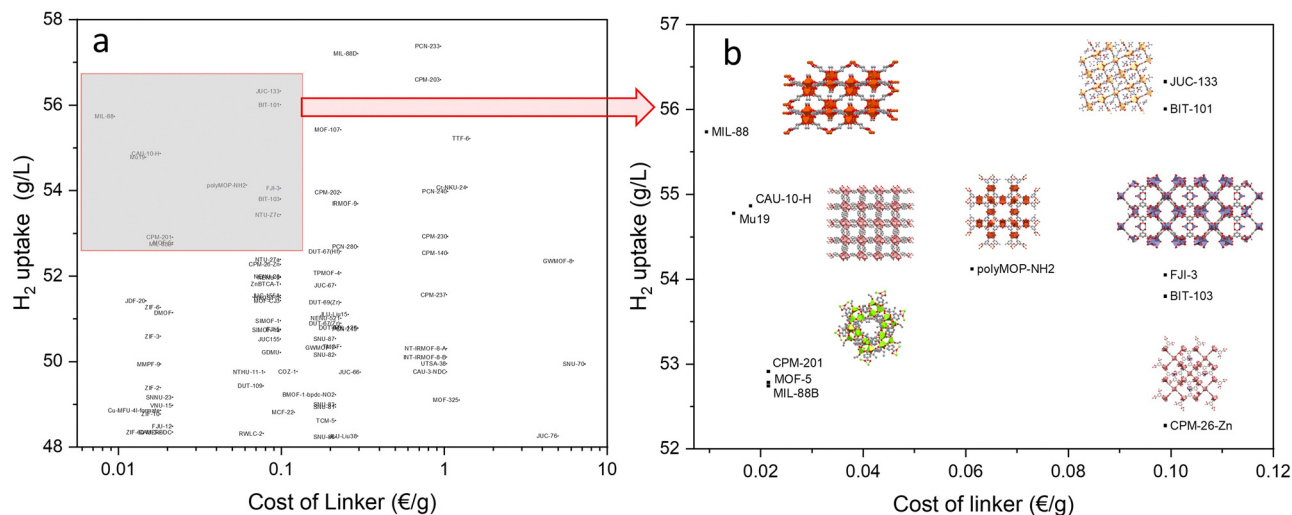


Fig. 3 (a) Volumetric hydrogen uptake of MOFs from single linkers cheaper than  $10 \text{ € kg}^{-1}$ . (b) Selection corresponding to cheapest linkers and best performance.

The most common linker-metal combination is  $\text{H}_2\text{BDC}$  and Zn, yielding 32 different entries in the database (Table S1 in the ESI†) and constituting one of the cheapest combinations of metal-linkers to synthesise MOFs. This combination is used in the archetypal MOF-5 (CSD code MIQBAR), one of the porous materials with the highest measured volumetric hydrogen uptake by cryoadsorption.<sup>14,15</sup> The material  $\text{Zn}_3\text{-BDC}_4$  (UFE-NAW) is an interpenetrated network which could store the highest amount of hydrogen per volume ( $62 \text{ g L}^{-1}$ ) among terephthalate-based MOFs according to our estimation.

Many Zn-carboxylate MOFs, *e.g.*, MOF-5, show stability problems in contact with ambient moisture because of the weakness of the coordination bond between soft Lewis bases, like divalent metals, with hard Lewis acids, like carboxylates.<sup>34</sup> Stronger bonds are supposed to be formed when high-valence transition metal cations (like  $\text{Al}^{3+}$ ,  $\text{Cr}^{3+}$ ,  $\text{Fe}^{3+}$ ,  $\text{Ti}^{4+}$  or  $\text{Zr}^{4+}$ ) are coordinated with carboxylate linkers, or when N-donor linkers like azolates and pyridines (hard Lewis bases) coordinate divalent metal cations like  $\text{Co}^{2+}$ ,  $\text{Ni}^{2+}$ ,  $\text{Cu}^{2+}$  and  $\text{Zn}^{2+}$ . For this

reason, combinations of terephthalic acid with V, Mn, and Zr, with higher oxidation numbers than  $\text{Zn}^{2+}$ , might yield more robust structures in contact with water, for example, as a pollutant in hydrogen from electrolysis. Potentially stable structures with remarkable storage capacities in this database are MIL-88 and -88B (Fig. 4a), showing OMS of Fe, and UIO-66 (Fig. S4b in the ESI†) is a Zr-MOF known for its exceptional mechanical and hydrothermal stability.<sup>35</sup> Besides, materials MIL-53 and -101 are made of trivalent metals Cr and Al, showing improved stability,<sup>36</sup> and could store between 42 and  $45 \text{ g L}^{-1}$  of hydrogen according to our estimation.

However, even unstable MOFs (*i.e.*, MOF-5, MOF-177, *etc.*) can be interesting for hydrogen storage because the mechanical robustness of the structure is the only relevant parameter affecting the pressure cycling operation of the MOF, whether the material is not affected by its chemical instability during its handling.<sup>37</sup> In this sense, Moghadam and co-workers developed a machine-learning-based algorithm to predict the mechanical properties from topologies and structural

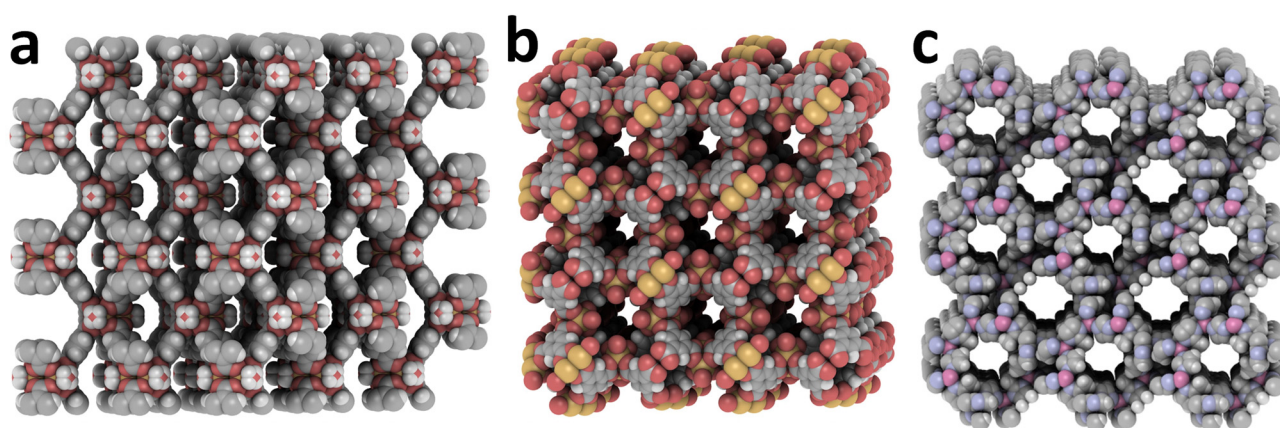


Fig. 4 (a) MIL-88B (Fe-BDC, CSD code KUXREC). (b)  $\text{Fe}_6\text{-BTC}_3$  (NINVAI). (c)  $\text{Cd-Melm}_2$  (GUPCAW). Created with iRASPA.<sup>39</sup>



properties.<sup>38</sup> Generally speaking, the bulk modulus diminishes for a specific topology of a MOF when the sizes of the cavities increase, therefore, materials with large volumetric areas but reduced specific areas are more desirable.

The second most common linker is H<sub>3</sub>BTC, most frequently linked to Cu in up to 25 structures of this database. Many entries correspond to the material HKUST-1 or Cu-BTC (DIH-VIB), one of the first MOFs tested for hydrogen adsorption.<sup>40</sup> Structures Zn<sub>2</sub>-BTC (RIZXUT) and Cd<sub>2</sub>-BTC (QISNAJ) show the highest estimated volumetric uptake. The structure Fe<sub>6</sub>-BTC<sub>3</sub> (Fig. 4b) is similar to that in HKUST-1 and exhibits OMS. This structure could show higher stability, as well as structures like Mn<sub>2</sub>-BTC (FUTCAZ), Mn<sub>3</sub>-BTC<sub>2</sub> (DEPXOM), and Cr<sub>3</sub>-BTC<sub>2</sub> (ZIG-FIG), with higher storage density than 50 g L<sup>-1</sup>.

The third most frequent linker is 2,5-dihydroxybenzene-1,4-dicarboxylic acid (H<sub>2</sub>DOTP), used to synthesise materials M-MOF-74/M-CPO-27/M-DOTP, where metals connected by oxygen atoms from the linker form rod-like metallic clusters and one-dimensional hexagonal channels.<sup>40</sup> These OMS-rich materials involve a high interaction with hydrogen molecules, reaching 13.5–15 kJ mol<sup>-1</sup>,<sup>27,41</sup> the highest measured enthalpy of adsorption among physisorbents. The hydrogen uptake of material with Zn in this database is 47 g L<sup>-1</sup>, but it could be underestimated because of the actual higher superficial packing density of the adsorbed hydrogen over this surface with a high concentration of OMS.<sup>42</sup>

Four structures have a potential storage capacity higher than 50 g L<sup>-1</sup> when using 2,6-naphthalenedicarboxylic acid (H<sub>2</sub>NDC) coordinated with Zn nodes. The 3D connected pores of the aluminium-based material CAU-3-NDC (Fig. S5a in the ESI†) could potentially store almost 50 g L<sup>-1</sup> but with higher physicochemical stability due to the higher hydrophobicity of the NDC linker and the presence of Al<sup>3+</sup> cations.<sup>43</sup>

All MOFs from H<sub>3</sub>BTB contain divalent metals, then structures with low stability are expected. However, this expansion of the linker BTC generates ultraporous structures like MOF-177 (Zn<sub>2</sub>-BTB or VOLRAQ) or MOF-14 (Cu<sub>3</sub>-BTB<sub>2</sub> or QOWQUO), which could ideally store 50 g L<sup>-1</sup> of hydrogen and has been synthesised by a solvent-free ball-milling approach,<sup>44</sup> potentially reducing its production cost.

Thiophene-2,5-dicarboxylic acid (H<sub>2</sub>TDC) is the linker of material CPM-202 or Mg-TDC (TAGTED), which has been tested for CO<sub>2</sub> and CH<sub>4</sub> adsorption.<sup>32</sup> Using this linker, Zr-based materials DUT-69 (Fig. S5b in the ESI†) and DUT-67 (Fig. S5c in the ESI†) could store more than 50 g L<sup>-1</sup> within their probed permanent porosity.<sup>45</sup>

The linker 3,3',5,5'-azobenzenetetracarboxylic acid (H<sub>4</sub>AzBTC) is the most expensive one considered herein. This compound yields seven MOFs overpassing 50 g L<sup>-1</sup> of potential hydrogen capacity by coordinating divalent Cu, Cd, and Zn. The Cu-derivative JUC-62 (Cu<sub>4</sub>-AzBTC<sub>2</sub>, OFOCUI) meets both gravimetric and volumetric DOE goals according to experimental measurements.<sup>46</sup> However, the moisture stability could be higher for Fe-based MOFs PCN-250' (Fig. 5), whose volumetric hydrogen uptake was measured as 53 g L<sup>-1</sup> considering the measured density of the crystals.<sup>31</sup> Similar structures like

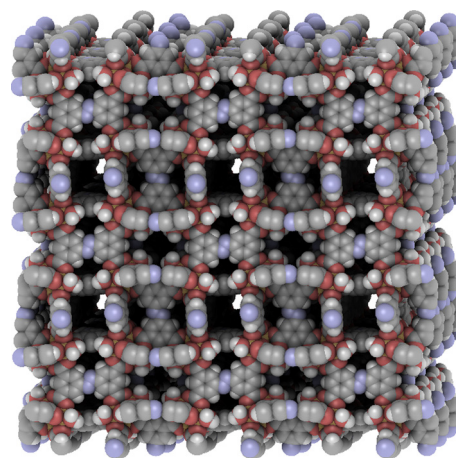


Fig. 5 PCN-250' or Fe<sub>2</sub>-AzBTC (CSD code TOWPEC). Created with iRASPA.<sup>39</sup>

Fe<sub>6</sub>-AzTBC<sub>3</sub> and Al<sub>6</sub>-AzBTC<sub>3</sub> could also show high stability to moisture as well.

The linker 4,4'-biphenyldicarboxylic acid (H<sub>2</sub>bPDC) is present in the structure UIO-67 (WIZMAV02), a Zr-based MOF isorecticular to UIO-66 (see Fig. S4b in the ESI†) whose expanded linker enhances the surface area and pore volume as well as the hydrogen adsorption uptake.<sup>47</sup> Despite the presence of Zr as a metal, poor stability after ambient exposure was detected in UIO-67,<sup>31</sup> probably because the used linker is larger than that of UIO-66.<sup>34</sup>

The most used N-donor linker is 4,4'-bipyridine (4,4'bPy), usually mixed with other linkers. However, there are some examples of single-linkers with Cu clusters like structures Cu-4,4'bPy<sub>2</sub> (Fig. S6 in the ESI†), where nitrogen atoms from the linker occupy the four positions in each square-plane in the Cu-octahedron, coordinating solvent molecules in the axial positions and yielding structures with square-section channels. These structures could also show OMS if they are stable after removing the coordinated solvent molecules.

2-Methylimidazole (HMeIm) is the most used azolate derivative in this selection, obtaining ZIF compounds (zeolitic imidazolate frameworks) when coordinating Me<sup>2+</sup> cations. The most known ZIF representative, commercially available, is the Zn-based material ZIF-8 (Fig. S7a in the ESI†) with zeolitic SOD topology, which was one of the first examples of MOF with ultra-high thermal and chemical stabilities.<sup>48</sup> The Cd-derivative Cd-MeIm<sub>2</sub> (Fig. 4c), with a zeolitic MER topology,<sup>49</sup> shows the highest potential for volumetric hydrogen storage (*ca.* 50 g L<sup>-1</sup>). Imidazole (Him) is the next most frequently used azole, like in the GIS-type structures Zn-Im<sub>2</sub> ZIF-6, ZIF-3, and ZIF-2. Up to 12 structures are deposited starting from 5-(4-pyridyl)tetrazol (PTz) as a linker, where Cu-PTz (Fig. S7c in the ESI†) potentially shows the highest hydrogen storage density (51 g L<sup>-1</sup>).

Pyridine-3,5-dicarboxylic acid (H<sub>2</sub>3,5PyDC) or dinicotinic acid simultaneously acts as an N- and O-donor linker so that the stability of the resulting frameworks in acidic or basic media might be lower than that for a purely N- or O-donor linker, depending on the present metal.<sup>34</sup> However, the stability



against ambient moisture could be enhanced because the structure has one strong Me-linker bond (with either N- or O-donor groups). The structure Zn-3,5PyDC (Fig. S8a in the ESI†) could potentially store up to 60 g L<sup>-1</sup> of H<sub>2</sub> if the structure is stable after removing the coordinated DMF molecules from Zn tetrahedra. Material JLU-Liu15 (Fig. S8b in the ESI†) shows a structure similar to material HKUST-1 and was used for selective adsorption of CO<sub>2</sub>.<sup>50</sup> Another pyridine derivative, pyridine-4-carboxamide (P4CA) or isonicotinic acid, yields structures with OMS Cd-P4CA (ROCZAM and UMABIV) with higher estimated uptake than 50 g L<sup>-1</sup>.

Besides pure linker MOFs, it is possible to find structures mixing more than one linker to coordinate single or mixed metal cations with remarkable volumetric hydrogen storage uptakes. Mixing linkers could be a cheaper alternative than developing new linkers for constructing new MOF frameworks, opening new opportunities for structural versatility. Indeed, mixed-linker materials UCMC-1, UCMC-2, UCMC-3, MOF-205, and MOF-210 exhibit some of the highest reported porous properties.<sup>15</sup> Herein, 224 MOFs are selected from the combination of two linkers cheaper than H<sub>4</sub>AzBTC and up to two metals. Structures with a third organic molecule are not selected, then those using extra-framework species like charge-balancing ions, structure-directing agents, or templates are not considered.

Fig. 6 compares the hydrogen uptake of MOFs resulting from the combination of the cheapest linkers. MOFs without a label are compounds without a name, for which only the CSD code is available. The highest concentration of the deposited structures corresponds to the combinations of cheaper linkers to 0.2 € g<sup>-1</sup>, whose highest uptakes correspond to materials DMOF and NENU-28. Other structures with lower calculated volumetric uptake than 50 g L<sup>-1</sup> made from the cheapest linkers are PTC-33, SNNU-22, JUC-65, -66, -67 and 85-a; DUT-67(Zr), MCF-36 and -37, PMOF-55, 4-pyCN@MIL-88B, and CPM-420.

There is no data about the permanent porosity, gas adsorption performance, or structural stability of many of these MOFs. They use either the same or different coordinating moieties in their linkers, like those combining O- and N-donor groups from, *e.g.*, carboxylates or pyridines. Tables from S16 to S21 in the ESI† show the minimum hydrogen uptake reached by the most interesting combinations of metals and linkers, considering the nature of the coordination moieties, which could affect the material's stability. Among the selected 19 interesting combinations of O-donor linkers, ten involve divalent metals like Zn. The highest uptake of 53.6 g L<sup>-1</sup> was calculated for the combination of H<sub>2</sub>BDC and serine (Ser) with Zn, corresponding to the structure Zn<sub>4</sub>-BDC-Ser<sub>2</sub> (RAPYOY). Using H<sub>2</sub>bPDC instead of Ser drives the formation of Zn<sub>4</sub>-BDC<sub>2</sub>-bPDC (FECZAQ), where DMF and water molecules occupy the unsaturated sites in the metallic nodes by the linkers, potentially creating OMS. H<sub>2</sub>TDC and 4,4',4''-nitritotribenzoic acid (H<sub>3</sub>NOTB) coordinate Zn<sub>4</sub>O clusters and could also exhibit OMS in the material NENU-521 or Zn<sub>20</sub>-TDC<sub>3</sub>-NOTB<sub>8</sub> (ZACHET). In structure Cd<sub>6</sub>-BTC<sub>4</sub>-BDC (EWECOY), H<sub>2</sub>BDC and H<sub>3</sub>BTC coordinate helicoidal chains of Cd atoms reaching almost 50 g L<sup>-1</sup>. All these structures are Zn-carboxylates, which could show the same problems of instability to moisture as the single-linker analogous Zn-carboxylate MOFs. However, coordinating octa-core aluminium-oxide clusters might show higher stability using a combination of the linker H<sub>3</sub>BTB with H<sub>2</sub>FA in structure MOF-520 (Fig. 7a), tested for methane storage.<sup>51</sup>

The mixture of purely N-donor linkers with divalent Zn or Cu metals produces potentially highly stable materials for water exposure and basic media. However, higher uptakes are predicted when N-donor and O-donor linkers are mixed in a MOF structure. The mixture of N- and O-donor functionalities has an unpredictable effect on materials' stability, and this aspect should be tested for each structure. For example, mixing benzene-1,3-dicarboxylic acid (H<sub>2</sub>IA) and 3,5-dimethyl-1,2,4-triazole (3,5dMeTz) produces the structure MAC-8 (Fig. S9a in

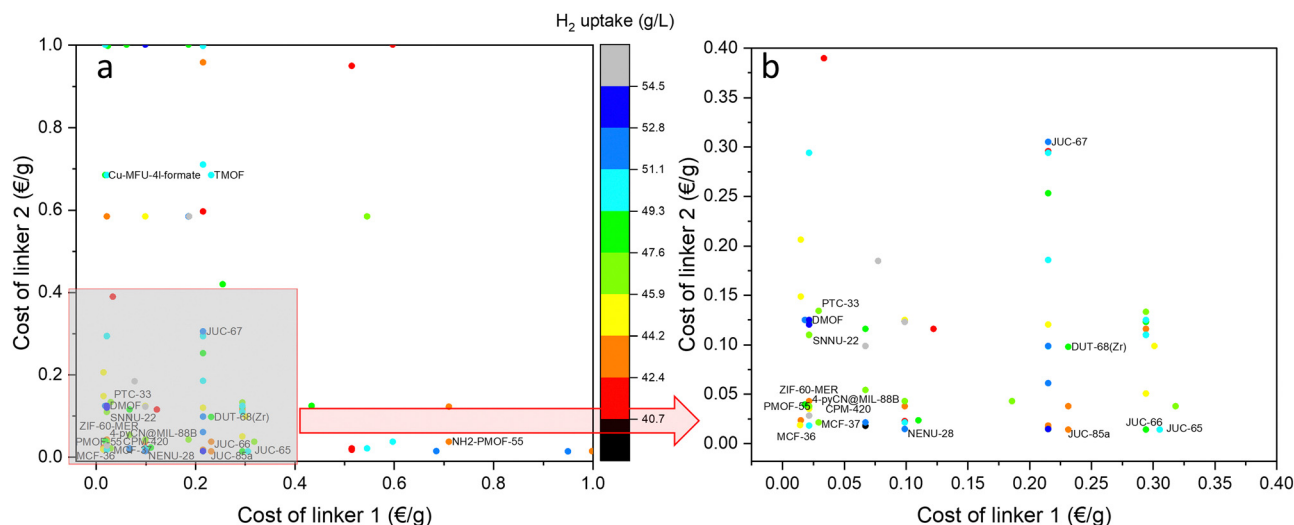


Fig. 6 (a) Comparison of hydrogen uptakes at  $-197^{\circ}\text{C}$  and 100 bar of MOFs made from the binary combinations of cheaper linkers than 1 € g<sup>-1</sup>. (b) Selection of structures from the cheapest linkers.





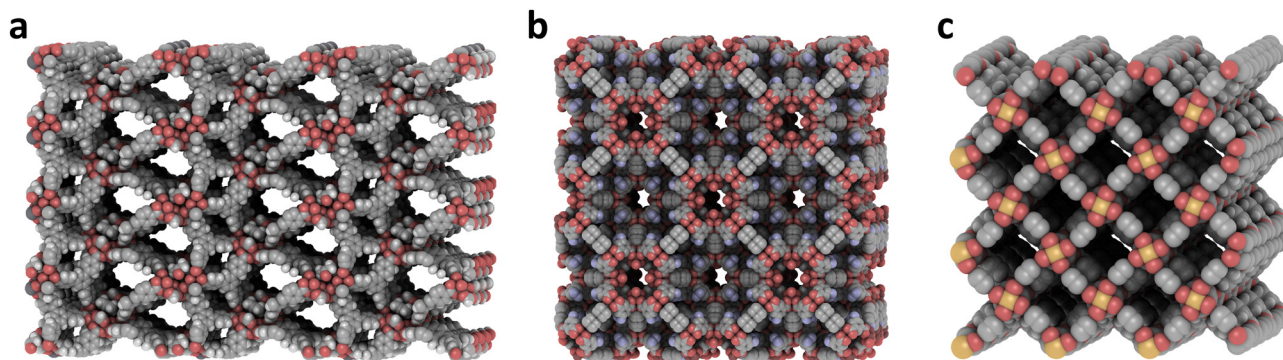


Fig. 7 (a) MOF-520 or  $\text{Al}_2\text{-BTB-FA}$  (RIXPIZ). (b)  $\text{Zn}_2\text{-PyEty-OBZ}_2$  (DIDDOK). (c)  $\text{Fe}_2\text{-BDC}_2\text{-DABCO}$  (XIVVEF). Created with iRASPA.<sup>39</sup>

the ESI†) with  $50.4 \text{ g L}^{-1}$  of hydrogen uptake. Mixing  $\text{H}_3\text{BTC}$  and benzotriazole (BTrz) yields structures  $\text{Zn}_9\text{-BTC}_6\text{-BTrz}_3$  (Fig. S9b in the ESI†) and  $\text{Zn}_3\text{-BTC}_2\text{-BTrz}$  (NESVEO) with a minimum uptake of  $52.7 \text{ g L}^{-1}$ . Mixing 4,4'-ethene-1,2-diylidibenzoic acid ( $\text{H}_2\text{EDB}$ ) and 1,2,4-triazole (1,2,4TrAz) generates the structure MAC-14 (Fig. S9c in the ESI†) with the potential to store  $50.9 \text{ g L}^{-1}$  of hydrogen.

From the 32 combinations of carboxylate acids and bipyridines, those using 2,2'-bipyridyl (2,2'bPy) as an N-donor linker usually yield structures where  $\text{Me-2,2'bPy}$  clusters occupy the MOF cavities and reduce the available pore volume. This possibility is reduced when using 4,4'bPy because the distance between nitrogen atoms in the linker is maximised, increasing the possibilities for creating a porous coordination polymer instead of metal chelates. Combining 4,4'bPy with 5-aminobenzene-1,3-dicarboxylic acid ( $\text{H}_2\text{NIA}$ ) and Cu generates the structure  $\text{Cu}_4\text{-NIA}_4\text{-4,4'bPy}$  (Fig. 8a) with open tridimensional porosity and potential OMS. In combination with  $\text{H}_2\text{bPDC}$  acid and Cu, the tridimensionally porous catenated structure  $\text{Cu}_2\text{-bPDC}_2\text{-4,4'bPy}$  (EDOMAM) is obtained. The combination with 3,4-pyridinedicarboxylic acid ( $\text{H}_2\text{3,4PyDC}$ ) and Cd creates the material JUC-67 (Fig. S8b in the ESI†), whose permanent porosity can allocate 12 methanol molecules per unit cell.<sup>52</sup> Finally, the combination with  $\text{H}_2\text{DOTP}$  and Zn ( $\text{Zn-DOTP-4,4bPy}$ , SUPLOF) can potentially store  $50.2 \text{ g L}^{-1}$  of hydrogen.

Twenty-seven combinations of carboxylates and other pyridine or pyrazine derivatives yield mixed linkers MOFs with potentially high hydrogen storage density, like structure

$\text{Zn}_3\text{Cr}_3\text{-BDC}_3\text{-P4CA}_6$  (XODPUD). If  $\text{H}_3\text{BTC}$  is used as the carboxylate linker, structure  $\text{Zn}_3\text{Cr}_3\text{-BTC}_2\text{-P4CA}_6$  (SETSIV) is obtained with an even higher storage density. The synthesised material  $\text{Zn}_2\text{-PyEty-OBZ}_2$  (Fig. 8c) from 4,4'-oxydibenzoic acid ( $\text{H}_2\text{ODBZ}$ ) and 1,2-bis(4-pyridyl)ethylene (PyEty) shows a highly porous three-dimensional network containing large cavities of about  $13.11 \text{ \AA}^3$ ,<sup>53</sup> for which  $55.7 \text{ g L}^{-1}$  of stored hydrogen density is estimated. Structure  $\text{Cu}_4\text{-5OIA}_4\text{-Pyz}$  (NIMQAD) from 5-hydroxybenzene-1,3-dicarboxylic acid ( $\text{H}_2\text{5OIA}$ ) and pyrazine (Pyz) linking Cu-paddle wheel clusters could store  $51.2 \text{ g L}^{-1}$  of hydrogen in a similar framework into the material shown in Fig. 7b. Structure  $\text{Zn}_2\text{-tBuIA-PyEt}$  (NUMPAO) from 5-*tert*-butylbenzene-1,3-dicarboxylic acid ( $\text{H}_2\text{tBuIA}$ ) and 1,2-bis(4-pyridyl)ethane (PyEt) could store  $53 \text{ g L}^{-1}$  of hydrogen. Finally,  $\text{H}_3\text{BTB}$  and P4CA coordinate Zn and Cr atoms to generate the structure  $\text{Cr}_3\text{Zn}_3\text{-BTB}_2\text{-P4CA}_6$  (SETSUH) with an uptake of  $50.6 \text{ g L}^{-1}$ . Some MOFs combine carboxylate-based and N-donor linkers like purines, diazabicyclo or hexamethyltetraamino compounds. For example, 1,4-diazabicyclo[2.2.2]octane (DABCO) and  $\text{H}_2\text{IA}$  coordinating Zn-oxide clusters in a paddle-wheel configuration yield the structure  $\text{Zn}_4\text{-IA}_4\text{-DABCO}$  (FORXAM, similar to Fig. 7b) which could store  $51.9 \text{ g L}^{-1}$  of hydrogen. If  $\text{H}_2\text{BDC}$  is used to coordinate Zn, the material  $\text{Zn}_2\text{-BDC}_2\text{-DABCO}$  (Fig. S10-a in the ESI†) could store  $52.5 \text{ g L}^{-1}$  of hydrogen, the same uptake as  $\text{CuZn-BDC}_2\text{-DABCO}$  (WARFIG).  $\text{Fe}_2\text{-BDC}_2\text{-DABCO}$  (Fig. 7c) and  $\text{Ni-BDC}_2\text{-DABCO}$  (EZOFUV) store  $51.6$  and  $50.3 \text{ g L}^{-1}$  of hydrogen, respectively. If  $\text{H}_2\text{bPDC}$  substitutes the cheaper  $\text{H}_2\text{BDC}$ , the material  $\text{Zn}_2\text{-bPDC}_2\text{-}$

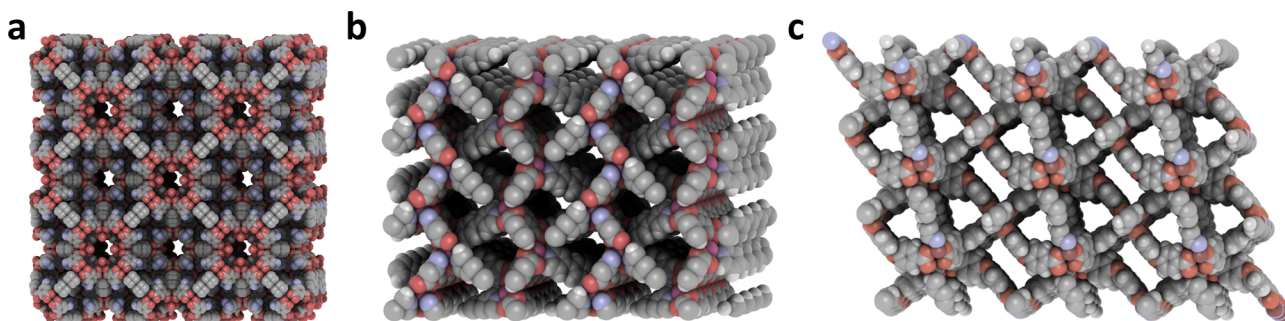


Fig. 8 (a)  $\text{Cu}_4\text{-NIA}_4\text{-4,4'bPy}$  (CSD code IVEKEA). (b) JUC-67 or  $\text{Cd}_2\text{-4,4'bPy-3,4PyDC}_2$  (HOWQAM). (c)  $\text{Zn}_2\text{-PyEty-OBZ}_2$  (DIDDOK). Created with iRASPA.<sup>39</sup>



DABCO (FEFDEB) could store  $50.6 \text{ g L}^{-1}$  of hydrogen. Also more expensive but still within the selected feasibility criteria, the combination of DABCO with 4,4'-carbonyldibenzoic acid ( $\text{H}_2\text{4,4'CODB}$ ) results in structure  $\text{Zn}_2\text{-4,4'CODB}_2\text{-DABCO}$  (Fig. S10-b in the ESI†), and with 4,4'-(1,1,1,3,3,3-hexafluoropropane-2,2-diyl)dibenzoic acid ( $\text{H}_2\text{F}_6\text{PdB}$ ) in  $\text{Zn}_2\text{-F}_6\text{PdB}_2\text{-DABCO}$  (WIH-WAN), both potentially storing  $51 \text{ g L}^{-1}$  of hydrogen.

## Conclusions

Herein, we elaborated a database of *ca.* 3500 structures from the CoRE MOF database obtained from industrially relevant metals, further estimating their hydrogen uptake. Structures with higher uptake than  $40 \text{ g L}^{-1}$  at 77 K and 100 bar, predicted from their calculated porous properties, were selected. The database collects the organic composition of materials, together with crystallographic, structural, chemical, and porous properties. Finally, the cost-per-gram of the organic linkers, if they are commercially available, is also collected and used to compare the feasibility of structures for their industrial production. We found that high volumetric storage density can be achieved using inexpensive linkers, like terephthalic or trimesic acids, alone or combined with affordable linkers and metals.

Up to 666 MOF structures from individual linkers and metals can show successful operation for volumetric hydrogen storage using linkers cheaper than  $\text{H}_4\text{AzBTC}$ , the linker of the commercially available material PCN-250(Fe). Carboxylate MOFs coordinating divalent metals like Zn or Cu are more commonly reported, like those found in MOF-5 and HKUST-1. However, the structural stability after moisture exposition could be enhanced using trivalent or tetravalent metals like Al or Zr.

Mixing metals and linkers increases the structural variety of MOFs. 224 promising MOF structures constructed from combinations of up to two linkers and two metals are collected in this database. Specially, combining linkers with N- and O-donor functionalities improves the porous properties with respect to the N-donor ones and may enhance the stability of the metal-organic bonds. Mixing carboxylates with azolates, pyridine, or pyrazine derivatives also drives the synthesis of potentially affordable porous MOF structures.

Beyond the selection of materials for hydrogen adsorption, this database opens the possibility of selecting affordable structures for different applications where porosity, crystallinity or composition are relevant parameters. Also, it facilitates the creation of derivatives from existing MOFs by modifying their chemical composition, or even the development of new MOF structures from economically feasible components. Finally, the provided user interface allows the creation of customised MOF selections that can be useful to finding promising structures for these applications considering the properties of structures and linkers.

## Author contributions

JAV was the conceptual author of this work and performed the bibliographic research, the search of information, data

curation and formal analysis. MB performed the online database. NG contributed to the search of information about linkers. FE and MM supervised the work and provided funding support. All authors contributed to writing and validation of the manuscript.

## Conflicts of interest

The authors declare that there is no conflict of interest.

## Acknowledgements

This project has received funding from the German Federal Ministry of Economic Affairs and Climate Action and the EMPIR programme co-financed by the Participating States and from the European Union's Horizon 2020 research and innovation programme for supporting the project MefHySto (19ENG03).

## References

- 1 S. Dutta, A review on production, storage of hydrogen and its utilization as an energy resource, *J. Ind. Eng. Chem.*, 2014, **20**(4), 1148–1156, DOI: [10.1016/j.jiec.2013.07.037](https://doi.org/10.1016/j.jiec.2013.07.037); J. Rissman, C. Bataille, E. Masanet, N. Aden, W. R. Morrow, N. Zhou, N. Elliott, R. Dell, N. Heeren and B. Huckestein, *et al.*, Technologies and policies to decarbonize global industry: Review and assessment of mitigation drivers through 2070, *Appl. Energy*, 2020, **266**, 114848, DOI: [10.1016/j.apenergy.2020.114848](https://doi.org/10.1016/j.apenergy.2020.114848).
- 2 U. Eberle, M. Felderhoff and F. Schuth, Chemical and physical solutions for hydrogen storage, *Angew. Chem., Int. Ed.*, 2009, **48**(36), 6608–6630, DOI: [10.1002/anie.200806293](https://doi.org/10.1002/anie.200806293).
- 3 J. Andersson and S. Gronkvist, Large-scale storage of hydrogen, *Int. J. Hydrogen Energy*, 2019, **44**(23), 11901–11919, DOI: [10.1016/j.ijhydene.2019.03.063](https://doi.org/10.1016/j.ijhydene.2019.03.063).
- 4 R. C. Lochan and M. Head-Gordon, Computational studies of molecular hydrogen binding affinities: the role of dispersion forces, electrostatics, and orbital interactions, *Phys. Chem. Chem. Phys.*, 2006, **8**(12), 1357–1370, DOI: [10.1039/b515409j](https://doi.org/10.1039/b515409j).
- 5 E. Poirier and A. Dailly, On the nature of the adsorbed hydrogen phase in microporous metal-organic frameworks at supercritical temperatures, *Langmuir*, 2009, **25**(20), 12169–12176, DOI: [10.1021/la901680p](https://doi.org/10.1021/la901680p).
- 6 L. Zhou, Y. P. Zhou and Y. Sun, Enhanced storage of hydrogen at the temperature of liquid nitrogen, *Int. J. Hydrogen Energy*, 2004, **29**(3), 319–322, DOI: [10.1016/S0360-3199\(03\)00155-1](https://doi.org/10.1016/S0360-3199(03)00155-1).
- 7 M. Schlichtenmayer and M. Hirscher, Nanosponges for hydrogen storage, *J. Mater. Chem.*, 2012, **22**(20), 10134–10143, DOI: [10.1039/c2jm15890f](https://doi.org/10.1039/c2jm15890f); M. Hirscher, V. A. Yartys, M. Baricco, J. B. von Colbe, D. Blanchard, R. C. Bowman, D. P. Broom, C. E. Buckley, F. Chang and P. Chen, *et al.*, Materials for hydrogen-based energy storage – past, recent progress and future outlook, *J. Alloys Compd.*,



- 2020, **827**, 153548, DOI: [10.1016/j.jallcom.2019.153548](https://doi.org/10.1016/j.jallcom.2019.153548); K. M. Thomas, Adsorption and desorption of hydrogen on metal-organic framework materials for storage applications: comparison with other nanoporous materials, *Dalton Trans.*, 2009, 1487–1505, DOI: [10.1039/b815583f](https://doi.org/10.1039/b815583f); Z. J. Chen, K. O. Kirlikovali, K. B. Idrees, M. C. Wasson and O. K. Farha, Porous materials for hydrogen storage, *Chem*, 2022, **8**(3), 693–716, DOI: [10.1016/j.chempr.2022.01.012](https://doi.org/10.1016/j.chempr.2022.01.012); L. Zhang, M. D. Allendorf, R. Balderas-Xicohtencatl, D. P. Broom, G. S. Fanourgakis, G. E. Froudakis, T. Genett, K. Hurst, S. Ling and C. Milanese, Fundamentals of hydrogen storage in nanoporous materials, *Prog. Energy*, 2022, **4**(4), 042013, DOI: [10.1088/2516-1083/ac8d44](https://doi.org/10.1088/2516-1083/ac8d44).
- 8 S. R. Batten, N. R. Champness, X. M. Chen, J. Garcia-Martinez, S. Kitagawa, L. Ohrstrom, M. O'Keeffe, M. P. Suh and J. Reedijk, Terminology of metal-organic frameworks and coordination polymers (IUPAC Recommendations 2013), *Pure Appl. Chem.*, 2013, **85**(8), 1715–1724, DOI: [10.1351/Pac-Rec-12-11-20](https://doi.org/10.1351/Pac-Rec-12-11-20); M. O'Keeffe and O. M. Yaghi, Deconstructing the crystal structures of metal-organic frameworks and related materials into their underlying nets, *Chem. Rev.*, 2012, **112**(2), 675–702, DOI: [10.1021/cr200205j](https://doi.org/10.1021/cr200205j).
  - 9 P. Z. Moghadam, A. Li, S. B. Wiggin, A. Tao, A. G. P. Maloney, P. A. Wood, S. C. Ward and D. Fairen-Jimenez, Development of a Cambridge Structural Database Subset: A Collection of Metal–Organic Frameworks for Past, Present, and Future, *Chem. Mater.*, 2017, **29**(7), 2618–2625, DOI: [10.1021/acs.chemmater.7b00441](https://doi.org/10.1021/acs.chemmater.7b00441).
  - 10 S. S. Kaye, A. Dailly, O. M. Yaghi and J. R. Long, Impact of preparation and handling on the hydrogen storage properties of Zn<sub>4</sub>O(1,4-benzenedicarboxylate)<sub>3</sub> (MOF-5), *J. Am. Chem. Soc.*, 2007, **129**(46), 14176–14177, DOI: [10.1021/ja076877g](https://doi.org/10.1021/ja076877g).
  - 11 O. K. Farha, A. O. Yazaydin, I. Eryazici, C. D. Malliakas, B. G. Hauser, M. G. Kanatzidis, S. T. Nguyen, R. Q. Snurr and J. T. Hupp, De novo synthesis of a metal-organic framework material featuring ultrahigh surface area and gas storage capacities, *Nat. Chem.*, 2010, **2**(11), 944–948, DOI: [10.1038/nchem.834](https://doi.org/10.1038/nchem.834); H. Furukawa, N. Ko, Y. B. Go, N. Aratani, S. B. Choi, E. Choi, A. O. Yazaydin, R. Q. Snurr, M. O'Keeffe and J. Kim, *et al.*, Ultrahigh porosity in metal-organic frameworks, *Science*, 2010, **329**(5990), 424–428, DOI: [10.1126/science.1192160](https://doi.org/10.1126/science.1192160).
  - 12 J. Goldsmith, A. G. Wong-Foy, M. J. Cafarella and D. J. Siegel, Theoretical Limits of Hydrogen Storage in Metal-Organic Frameworks: Opportunities and Trade-Offs, *Chem. Mater.*, 2013, **25**(16), 3373–3382, DOI: [10.1021/cm401978e](https://doi.org/10.1021/cm401978e).
  - 13 R. Balderas-Xicohtencatl, M. Schlichtenmayer and M. Hirscher, Volumetric Hydrogen Storage Capacity in Metal–Organic Frameworks, *Energy Technol.*, 2018, **6**(3), 578–582, DOI: [10.1002/ente.201700636](https://doi.org/10.1002/ente.201700636).
  - 14 D. Zhao, D. Q. Yuan and H. C. Zhou, The current status of hydrogen storage in metal-organic frameworks, *Energy Environ. Sci.*, 2008, **1**(2), 222–235, DOI: [10.1039/b808322n](https://doi.org/10.1039/b808322n); J. Sculley, D. Q. Yuan and H. C. Zhou, The current status of hydrogen storage in metal-organic frameworks-updated, *Energy Environ. Sci.*, 2011, **4**(8), 2721–2735, DOI: [10.1039/c1ee01240a](https://doi.org/10.1039/c1ee01240a).
  - 15 M. P. Suh, H. J. Park, T. K. Prasad and D. W. Lim, Hydrogen storage in metal-organic frameworks, *Chem. Rev.*, 2012, **112**(2), 782–835, DOI: [10.1021/cr200274s](https://doi.org/10.1021/cr200274s).
  - 16 US Department of Energy, D. O. E. DOE Technical Targets for Onboard Hydrogen Storage for Light-Duty Vehicles. 2012. <https://www.energy.gov/eere/fuelcells/doe-technical-targets-onboard-hydrogen-storage-light-duty-vehicles> (accessed 2021 30/11/2021).
  - 17 C. E. Wilmer, M. Leaf, C. Y. Lee, O. K. Farha, B. G. Hauser, J. T. Hupp and R. Q. Snurr, Large-scale screening of hypothetical metal–organic frameworks, *Nat. Chem.*, 2012, **4**(2), 83–89, DOI: [10.1038/Nchem.1192](https://doi.org/10.1038/Nchem.1192); A. Ahmed, S. Seth, J. Purewal, A. G. Wong-Foy, M. Veenstra, A. J. Matzger and D. J. Siegel, Exceptional hydrogen storage achieved by screening nearly half a million metal-organic frameworks, *Nat. Commun.*, 2019, **10**(1), 1568, DOI: [10.1038/s41467-019-09365-w](https://doi.org/10.1038/s41467-019-09365-w).
  - 18 U. Ryu, S. Jee, P. C. Rao, J. Shin, C. Ko, M. Yoon, K. S. Park and K. M. Choi, Recent advances in process engineering and upcoming applications of metal-organic frameworks, *Coord. Chem. Rev.*, 2021, **426**, 213544, DOI: [10.1016/j.ccr.2020.213544](https://doi.org/10.1016/j.ccr.2020.213544); Z. Chen, M. C. Wasson, R. J. Drouot, L. Robison, K. B. Idrees, J. G. Knapp, F. A. Son, X. Zhang, W. Hierse and C. Kuhn, *et al.*, The state of the field: from inception to commercialization of metal-organic frameworks, *Faraday Discuss.*, 2021, **225**, 9–69, DOI: [10.1039/d0fd00103a](https://doi.org/10.1039/d0fd00103a).
  - 19 D. DeSantis, J. A. Mason, B. D. James, C. Houchins, J. R. Long and M. Veenstra, Techno-economic Analysis of Metal-Organic Frameworks for Hydrogen and Natural Gas Storage, *Energy Fuel*, 2017, **31**(2), 2024–2032, DOI: [10.1021/acs.energyfuels.6b02510](https://doi.org/10.1021/acs.energyfuels.6b02510); M. I. Severino, E. Gkaniatsou, F. Nouar, M. L. Pinto and C. Serre, MOFs industrialization: a complete assessment of production costs, *Faraday Discuss.*, 2021, **231**, 326–341, DOI: [10.1039/d1fd00018g](https://doi.org/10.1039/d1fd00018g).
  - 20 P. Peng, A. Anastasopoulou, K. Brooks, H. Furukawa, M. E. Bowden, J. R. Long, T. Autrey and H. Breunig, Cost and potential of metal-organic frameworks for hydrogen back-up power supply, *Nat. Energy*, 2022, **7**(5), 448–458, DOI: [10.1038/s41560-022-01013-w](https://doi.org/10.1038/s41560-022-01013-w).
  - 21 S. Bryant, Download scripts for the CSD Python API from the CSD GitHub repository, 2022, <https://www.ccdc.cam.ac.uk/Community/blog/download-csd-python-api-scripts-github/#how-to-use-csd-github-repo> (accessed 2022 2022-04-22); B. J. Bucior, A. S. Rosen, M. Haranczyk, Z. P. Yao, M. E. Ziebel, O. K. Farha, J. T. Hupp, J. I. Siepmann, A. Aspuru-Guzik and R. Q. Snurr, Identification Schemes for Metal-Organic Frameworks To Enable Rapid Search and Cheminformatics Analysis, *Cryst. Growth Des.*, 2019, **19**(11), 6682–6697, DOI: [10.1021/acs.cgd.9b01050](https://doi.org/10.1021/acs.cgd.9b01050).
  - 22 Y. G. Chung, J. Camp, M. Haranczyk, B. J. Sikora, W. Bury, V. Krungleviciute, T. Yildirim, O. K. Farha, D. S. Sholl and R. Q. Snurr, Computation-Ready, Experimental Metal-Organic Frameworks: A Tool To Enable High-Throughput



- Screening of Nanoporous Crystals, *Chem. Mater.*, 2014, **26**(21), 6185–6192, DOI: [10.1021/cm502594j](https://doi.org/10.1021/cm502594j).
- 23 Y. G. Chung, E. Haldoupis, B. J. Bucior, M. Haranczyk, S. Lee, H. D. Zhang, K. D. Vogiatzis, M. Milisavljevic, S. L. Ling and J. S. Camp, *et al.*, Advances, Updates, and Analytics for the Computation-Ready, Experimental Metal-Organic Framework Database: CoRE MOF 2019, *J. Chem. Eng. Data*, 2019, **64**(12), 5985–5998, DOI: [10.1021/acs.jced.9b00835](https://doi.org/10.1021/acs.jced.9b00835).
  - 24 J. A. Villajos, A. Zimathies and C. Prinz, A fast procedure for the estimation of the hydrogen storage capacity by cryoadsorption of metal-organic framework materials from their available porous properties, *Int. J. Hydrogen Energy*, 2021, **46**(57), 29323–29331, DOI: [10.1016/j.ijhydene.2020.10.265](https://doi.org/10.1016/j.ijhydene.2020.10.265).
  - 25 P. García-Holley, B. Schweitzer, T. Islamoglu, Y. Liu, L. Lin, S. Rodriguez, M. H. Weston, J. T. Hupp, D. A. Gómez-Gualdrón and T. Yildirim, *et al.*, Benchmark Study of Hydrogen Storage in Metal-Organic Frameworks under Temperature and Pressure Swing Conditions, *ACS Energy Lett.*, 2018, **3**(3), 748–754, DOI: [10.1021/acsenerylett.8b00154](https://doi.org/10.1021/acsenerylett.8b00154).
  - 26 W. Zhou, H. Wu and T. Yildirim, Enhanced H<sub>2</sub> adsorption in isostructural metal-organic frameworks with open metal sites: strong dependence of the binding strength on metal ions, *J. Am. Chem. Soc.*, 2008, **130**(46), 15268–15269, DOI: [10.1021/ja807023q](https://doi.org/10.1021/ja807023q).
  - 27 J. G. Vitillo, L. Regli, S. Chavan, G. Ricchiardi, G. Spoto, P. D. Dietzel, S. Bordiga and A. Zecchina, Role of exposed metal sites in hydrogen storage in MOFs, *J. Am. Chem. Soc.*, 2008, **130**(26), 8386–8396, DOI: [10.1021/ja8007159](https://doi.org/10.1021/ja8007159).
  - 28 R. Dalapati, B. Sakthivel, A. Dhakshinamoorthy, A. Buragohain, A. Bhunia, C. Janiak and S. Biswas, A highly stable dimethyl-functionalized Ce(IV)-based UiO-66 metal-organic framework material for gas sorption and redox catalysis, *CrystEngComm*, 2016, **18**(40), 7855–7864, DOI: [10.1039/c6ce01704e](https://doi.org/10.1039/c6ce01704e).
  - 29 Z. Chen, K. O. Kirlikovali, P. Li and O. K. Farha, Reticular Chemistry for Highly Porous Metal-Organic Frameworks: The Chemistry and Applications, *Acc. Chem. Res.*, 2022, **55**(4), 579–591, DOI: [10.1021/acs.accounts.1c00707](https://doi.org/10.1021/acs.accounts.1c00707).
  - 30 N. T. X. Huynh, V. Chihai and D. N. Son, Hydrogen storage in MIL-88 series, *J. Mater. Sci.*, 2019, **54**(5), 3994–4010, DOI: [10.1007/s10853-018-3140-4](https://doi.org/10.1007/s10853-018-3140-4).
  - 31 J. A. Villajos, Experimental Volumetric Hydrogen Uptake Determination at 77 K of Commercially Available Metal-Organic Framework Materials, *C*, 2022, **8**(1), 5, DOI: [10.3390/c8010005](https://doi.org/10.3390/c8010005).
  - 32 Q. G. Zhai, X. H. Bu, X. Zhao, C. Y. Mao, F. Bu, X. T. Chen and P. Y. Feng, Advancing Magnesium-Organic Porous Materials through New Magnesium Cluster Chemistry, *Cryst. Growth Des.*, 2016, **16**(3), 1261–1267, DOI: [10.1021/acs.cgd.5b01297](https://doi.org/10.1021/acs.cgd.5b01297).
  - 33 J. Bae, J. S. Choi, S. Hwang, W. S. Yun, D. Song, J. Lee and N. C. Jeong, Multiple Coordination Exchanges for Room-Temperature Activation of Open-Metal Sites in Metal-Organic Frameworks, *ACS Appl. Mater. Interfaces*, 2017, **9**(29), 24743–24752, DOI: [10.1021/acsami.7b07299](https://doi.org/10.1021/acsami.7b07299).
  - 34 S. Yuan, L. Feng, K. Wang, J. Pang, M. Bosch, C. Lollar, Y. Sun, J. Qin, X. Yang and P. Zhang, *et al.*, Stable Metal-Organic Frameworks: Design, Synthesis, and Applications, *Adv. Mater.*, 2018, **30**(37), e1704303, DOI: [10.1002/adma.201704303](https://doi.org/10.1002/adma.201704303).
  - 35 J. Winarta, B. Shan, S. M. McIntyre, L. Ye, C. Wang, J. Liu and B. Mu, A Decade of UiO-66 Research: A Historic Review of Dynamic Structure, Synthesis Mechanisms, and Characterization Techniques of an Archetypal Metal-Organic Framework, *Cryst. Growth Des.*, 2019, **20**(2), 1347–1362, DOI: [10.1021/acs.cgd.9b00955](https://doi.org/10.1021/acs.cgd.9b00955).
  - 36 I. Bezverkhyy, G. Weber and J. P. Bellat, Degradation of fluoride-free MIL-100(Fe) and MIL-53(Fe) in water: Effect of temperature and pH, *Microporous Mesoporous Mater.*, 2016, **219**, 117–124, DOI: [10.1016/j.micromeso.2015.07.037](https://doi.org/10.1016/j.micromeso.2015.07.037); M. Latroche, S. Surble, C. Serre, C. Mellot-Draznieks, P. L. Llewellyn, J. H. Lee, J. S. Chang, S. H. Jung and G. Férey, Hydrogen storage in the giant-pore metal-organic frameworks MIL-100 and MIL-101, *Angew. Chem. Int. Ed.*, 2006, **45**(48), 8227–8231, DOI: [10.1002/anie.200600105](https://doi.org/10.1002/anie.200600105).
  - 37 T. C. Wang, J. L. White, B. Bie, H. Deng, J. Edgington, J. D. Sugar, V. Stavila and M. D. Allendorf, Design Rules for Metal-Organic Framework Stability in High-Pressure Hydrogen Environments, *ChemPhysChem*, 2019, **20**(10), 1305–1310, DOI: [10.1002/cphc.201801190](https://doi.org/10.1002/cphc.201801190).
  - 38 P. Z. Moghadam, S. M. Rogge, A. Li, C.-M. Chow, J. Wieme, N. Moharrami, M. Aragones-Anglada, G. Conduit, D. A. Gomez-Gualdrón and V. Van Speybroeck, Structure-mechanical stability relations of metal-organic frameworks via machine learning, *Matter*, 2019, **1**(1), 219–234.
  - 39 D. Dubbeldam, S. Calero and T. J. H. Vlugt, iRASP: GPU-accelerated visualization software for materials scientists, *Mol. Simul.*, 2018, **44**(8), 653–676, DOI: [10.1080/08927022.2018.1426855](https://doi.org/10.1080/08927022.2018.1426855).
  - 40 J. L. Rowsell and O. M. Yaghi, Effects of functionalization, catenation, and variation of the metal oxide and organic linking units on the low-pressure hydrogen adsorption properties of metal-organic frameworks, *J. Am. Chem. Soc.*, 2006, **128**(4), 1304–1315, DOI: [10.1021/ja056639q](https://doi.org/10.1021/ja056639q).
  - 41 S. M. Chavan, O. Zavorotynska, C. Lamberti and S. Bordiga, H<sub>2</sub> interaction with divalent cations in isostructural MOFs: a key study for variable temperature infrared spectroscopy, *Dalton Trans.*, 2013, **42**(35), 12586–12595, DOI: [10.1039/c3dt51312b](https://doi.org/10.1039/c3dt51312b).
  - 42 Y. Liu, H. Kabbour, C. M. Brown, D. A. Neumann and C. C. Ahn, Increasing the density of adsorbed hydrogen with coordinatively unsaturated metal centers in metal-organic frameworks, *Langmuir*, 2008, **24**(9), 4772–4777, DOI: [10.1021/la703864a](https://doi.org/10.1021/la703864a); P. D. Dietzel, P. A. Georgiev, J. Eckert, R. Blom, T. Strassle and T. Unruh, Interaction of hydrogen with accessible metal sites in the metal-organic frameworks M(2)(dhtp) (CPO-27-M; M = Ni, Co, Mg), *Chem. Commun.*, 2010, **46**(27), 4962–4964, DOI: [10.1039/c0cc00091d](https://doi.org/10.1039/c0cc00091d).
  - 43 Z. W. Wang, M. Chen, C. S. Liu, X. Wang, H. Zhao and M. Du, A Versatile AlIII-Based Metal-Organic Framework with High Physicochemical Stability, *Chem. – Eur. J.*, 2015, **21**(48), 17215–17219, DOI: [10.1002/chem.201502615](https://doi.org/10.1002/chem.201502615).
  - 44 M. Klimakow, P. Klobes, A. F. Thunemann, K. Rademann and F. Emmerling, Mechanochemical Synthesis of Metal-





- Organic Frameworks: A Fast and Facile Approach toward Quantitative Yields and High Specific Surface Areas, *Chem. Mater.*, 2010, **22**(18), 5216–5221, DOI: [10.1021/cm1012119](https://doi.org/10.1021/cm1012119).
- 45 V. Bon, I. Senkovska, I. A. Baburin and S. Kaskel, Zr- and Hf-Based Metal-Organic Frameworks: Tracking Down the Polymorphism, *Cryst. Growth Des.*, 2013, **13**(3), 1231–1237, DOI: [10.1021/cg301691d](https://doi.org/10.1021/cg301691d).
  - 46 M. Xue, G. S. Zhu, Y. X. Li, X. J. Zhao, Z. Jin, E. Kang and S. L. Qiu, Structure, hydrogen storage, and luminescence properties of three 3D metal-organic frameworks with NbO and PtS topologies, *Cryst. Growth Des.*, 2008, **8**(7), 2478–2483, DOI: [10.1021/cg8001114](https://doi.org/10.1021/cg8001114).
  - 47 S. Chavan, J. G. Vitillo, D. Gianolio, O. Zavorotynska, B. Civalieri, S. Jakobsen, M. H. Nilsen, L. Valenzano, C. Lamberti and K. P. Lillerud, *et al.*, H<sub>2</sub> storage in isostructural UiO-67 and UiO-66 MOFs, *Phys. Chem. Chem. Phys.*, 2012, **14**(5), 1614–1626, DOI: [10.1039/c1cp23434j](https://doi.org/10.1039/c1cp23434j).
  - 48 K. S. Park, Z. Ni, A. P. Cote, J. Y. Choi, R. Huang, F. J. Uribe-Romo, H. K. Chae, M. O'Keeffe and O. M. Yaghi, Exceptional chemical and thermal stability of zeolitic imidazolate frameworks, *Proc. Natl. Acad. Sci. U. S. A.*, 2006, **103**(27), 10186–10191, DOI: [10.1073/pnas.0602439103](https://doi.org/10.1073/pnas.0602439103).
  - 49 Y. Q. Tian, S. Y. Yao, D. Gu, K. H. Cui, D. W. Guo, G. Zhang, Z. X. Chen and D. Y. Zhao, Cadmium imidazolate frameworks with polymorphism, high thermal stability, and a large surface area, *Chem. – Eur. J.*, 2010, **16**(4), 1137–1141, DOI: [10.1002/chem.200902729](https://doi.org/10.1002/chem.200902729).
  - 50 S. Surble, C. Serre, C. Mellot-Draznieks, F. Millange and G. Ferey, A new isorecticular class of metal-organic-frameworks with the MIL-88 topology, *Chem. Commun.*, 2006, 284–286, DOI: [10.1039/b512169h](https://doi.org/10.1039/b512169h).
  - 51 F. Gandara, H. Furukawa, S. Lee and O. M. Yaghi, High methane storage capacity in aluminum metal-organic frameworks, *J. Am. Chem. Soc.*, 2014, **136**(14), 5271–5274, DOI: [10.1021/ja501606h](https://doi.org/10.1021/ja501606h).
  - 52 M. Xue, G. S. Zhu, H. Ding, L. Wu, X. J. Zhao, Z. Jin and S. L. Qiu, Six Three-Dimensional Metal-Organic Frameworks with (3,4)-, (4,5)-, and (3,4,5)-Connected Nets Based on Mixed Ligands: Synthesis, Structures, and Adsorption Properties, *Cryst. Growth Des.*, 2009, **9**(3), 1481–1488, DOI: [10.1021/cg8009546](https://doi.org/10.1021/cg8009546).
  - 53 M. Kondo, Y. Irie, M. Miyazawa, H. Kawaguchi, S. Yasue, K. Maeda and F. Uchida, Synthesis and structural determination of new multidimensional coordination polymers with 4,4'-oxybis(benzoate) building ligands: Construction of coordination polymers with heteroorganic bridges, *J. Organomet. Chem.*, 2007, **692**(1–3), 136–141, DOI: [10.1016/j.jorganchem.2006.07.048](https://doi.org/10.1016/j.jorganchem.2006.07.048).

